Double Exchange via t_{2g} Orbitals and the Jahn-Teller Effect in Ferromagnetic $La_{0.7}Sr_{0.3}CoO_3$ Probed by Epitaxial Strain

D. Fuchs,[1] M. Merz,[1] P. Nagel,[1] R. Schneider,[1] S. Schuppler,[1] and H. von Löhneysen[1,2]

[1]*Institut für Festkörperphysik, Karlsruher Institut für Technologie, 76021 Karlsruhe, Germany*

[2]*Physikalisches Institut, Karlsruher Institut für Technologie, 76128 Karlsruhe, Germany*

(Received 19 July 2013; published 18 December 2013)

The magnetic exchange in hole-doped ferromagnetic cobaltates is investigated by studying the magnetic and electronic properties of $La_{0.7}Sr_{0.3}CoO_3$ films as a function of epitaxial strain. We found a strong-coupling double exchange mechanism between $Co^{3+}(4t_{2g}\ 2e_g)$ and $Co^{4+}(3t_{2g}\ 2e_g)$ high-spin states mediated by t_{2g} electrons—in contrast to the moderate coupling provided by the e_g exchange in manganites. The strong sensitivity of the Curie temperature T_C to the bulk compression can be explained by the small bandwidth of the t_{2g}-derived states. A strain-induced Jahn-Teller effect is likewise observed. The experimental results clarify the magnetic exchange mechanism in the cobaltates.

DOI: 10.1103/PhysRevLett.111.257203 PACS numbers: 75.70.−i, 75.30.Et, 75.47.Lx, 78.20.Ls

Transition-metal (TM) oxides with strong electronic correlations have attracted great attention in the past two decades owing to the discoveries of high-temperature superconductivity in layered cuprates and the colossal magnetoresistance in manganites. The perovskite cobaltates, with their evolution of the physical properties as a function of hole doping are, at first sight, very similar to the manganites [1]. Even though $La_{1-x}Sr_xCoO_3$ shows doping induced ferromagnetism and metallic behavior, the nature of the ferromagnetic state is rather unusual compared to that of $La_{1-x}Sr_xMnO_3$. Long-range ferromagnetic order is found for $x > 0.18$, whereas spin-glass and cluster-glass behavior are observed for lower x [2,3]. Additionally, the spin degree of freedom—due to the delicate balance between the crystal-field splitting Δ_{CF} and the exchange interaction J_{ex}—makes the cobaltates very unique and rich in magnetic states leading, e.g., to spin-state transitions [4] and strain-induced ferromagnetism in pure $LaCoO_3$ [5–8].

The most important scenarios which have been discussed for the dominant magnetic exchange in hole-doped perovskite cobaltates are the following: In a pioneering work, Goodenough [9] has proposed a modified superexchange or semicovalent exchange between Co^{3+} high spin (HS) and Co^{4+} low spin ions to describe the anomalous magnetic properties of $La_{1-x}Sr_xCoO_3$ without recourse to Zener's double-exchange (DE) mechanism [10,11], the most popular model to describe magnetism in perovskite-related oxides with differently ionized TM ions. However, recently published x-ray absorption measurements on $La_{1-x}Sr_xCoO_3$ indicate an exchange between t_{2g} derived states of Co^{3+} $(4t_{2g}\ 2e_g)$ HS and Co^{4+} $(3t_{2g}\ 2e_g)$ HS [12,13], which excludes the proposed exchange mechanism of Goodenough and Zener's double exchange mediated by e_g-derived states as observed for manganites. In a third scenario, a spin configuration fluctuation between Co^{3+} LS and Co^{3+} HS [14], as observed in strained $LaCoO_3$ [12], may be considered as well. However, the metallic character and the rather high T_C of $La_{0.7}Sr_{0.3}CoO_3$ (LSCO) compared to $LaCoO_3$ make that scenario very unlikely as a dominant one.

The strong hybridization between O $2p$ and the TM $3d$ orbitals leads to an appreciable charge transfer from Co to O [12,13]. Hence, structural distortions—such as tilting, rotation, or deformation of the regular CoO_6 octahedra—have a profound effect on the magnetic properties giving access to unravel correlations between structural and magnetic properties. This has motivated us to investigate the magnetic exchange in hole-doped LSCO films by studying the magnetic and electronic properties as a function of epitaxial strain. We show that a strong-coupling double exchange between Co^{3+} and Co^{4+} high-spin states via t_{2g} orbitals is the driving force for the ferromagnetic order in LSCO.

LSCO films were produced by pulsed laser deposition [15,16]. Epitaxially strained films were deposited with a film thickness of 40 nm under optimized growth conditions on ⟨001⟩ oriented $LaAlO_3$ (LAO), $(La_{0.7}Sr_{0.3})\times(Al_{0.65}Ta_{0.35})O_3$ (LSAT), and $SrTiO_3$ (STO). Rutherford backscattering spectrometry (RBS) confirmed the stoichiometric composition of the samples. Lattice parameters and strain were analyzed by x-ray diffraction (XRD). The magnetic properties of the films were studied using a superconducting quantum interference device system. X-ray absorption spectroscopy (XAS) and soft x-ray magnetic circular dichroism (XMCD) at the oxygen O K edge were performed at ≈ 20 K in total-electron-yield mode in an applied magnetic field of 7 T at the Institut für Festkörperphysik beam line WERA at the ANKA synchrotron light source (Karlsruhe, Germany). Spectra were taken at normal and grazing incidence of radiation with respect to the film surface. The energy resolution of the absorption spectra was set to 0.15 eV.

To produce homogeneously strained LSCO, pseudomorphic films were grown to a thickness of only 40 nm on substrates having a squarelike surface cell with in-plane

lattice parameter a_s close to that of LSCO. LSCO has a rhombohedral structure, R-3c, with a pseudocubic lattice parameter of $a_0 \approx 3.82$ Å [17]. The ferromagnetic order sets in at about 225 K [18,19]. The lattice mismatch of LSCO at room temperature amounts to -0.78%, 1.31%, and 2.09% for films on LAO, LSAT, and STO substrates, respectively. The strain states of the films are visualized by high-resolution XRD. Figure 1(a) displays reciprocal space maps of epitaxial LSCO films in the vicinity of the (103) substrate and LSCO film reflections. The LSCO films on LSAT and STO are fully strained, whereas the film on LAO displays minor relaxation [20] very likely along the twin boundaries of LAO due to the twinning below 500 °C after film deposition so that the most part of the surface layer is assumed to be still fully strained.

From the peak positions, we obtain the in- and out-of-plane lattice parameters a and c of the films, together with the lattice strain along the [100] and [001] directions at room temperature, i.e., $\varepsilon_{xx} = (a - a_0)/a_0$ and $\varepsilon_{zz} = (c - a_0)/a_0$. XRD measurements on bulk unstrained polycrystalline LSCO yield $a_0 = 3.822$ Å, consistent with literature [17]. Figure 1(b) shows ε_{xx} and ε_{zz} as a function of a_s. With increasing a_s, εxx increases as expected. Compressive strain ($\varepsilon_{xx} < 0$) is observed for $a_s < a_0$ (LSCO on LAO). ε_{xx} and ε_{zz} are compatible with a linear dependence on a_s. Strain-free films, i.e., $\varepsilon_{xx} = \varepsilon_{zz} = 0$, are not obtained probably due to the different thermal expansion coefficients of the film and substrate materials [6]. In Figure 1(c), ε_{zz} is plotted versus ε_{xx} demonstrating the linear relationship $\varepsilon_{zz} = c^* - \varepsilon_{xx}$, with $c^* = 0.83\%$.

The magnetic properties, i.e., the field-cooled magnetic moment $m(T)$ and hysteresis $m(H)$ are displayed in Figs. 1(d) and 1(e), respectively. T_C was determined by the minimum of the derivative dM/dT. The strained films display a T_C lower than that of bulk LSCO, decreasing successively with increasing ε_{xx} from 207 K for LSCO on LAO to $T_C = 171$ K for LSCO on STO. Unstrained polycrystalline LSCO shows a T_C of 220 K with an onset at 225 K. $m(H)$ curves were taken at $T = 15$ K, the temperature region where we also carried out the XMCD measurements. The coercive field $\mu_0 H_c$ increases with increasing tensile strain, reinforcing the in-plane magnetic easy axis by magnetoelastic anisotropy [21–23].

The electronic structure of the LSCO films was determined by XAS measurements at the Co $L_{2,3}$ edge and the O K edge. The Co $L_{2,3}$absorption spectra are very similar to each other and also to spectra previously taken from LSCO on STO [12]. The spectra taken at normal and grazing incidence do not display significant differences, indicating the homogeneity of the samples and the isotropic nature of the unoccupied electronic density of states. Since the spectral shape of the Co $L_{2,3}$ edge is strongly dominated by the valence and spin states of the involved Co ions, we conclude that the degree of charge-carrier doping and the spin state are hardly affected by epitaxial strain.

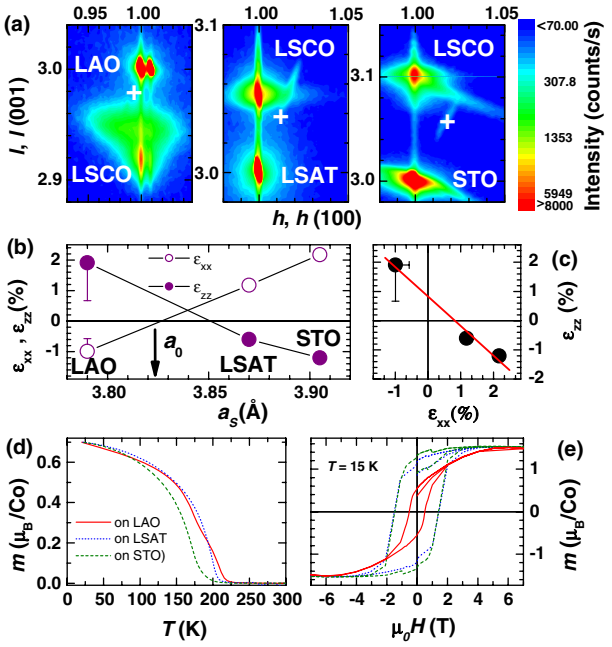

FIG. 1 (color online). (a) Reciprocal space maps of LSCO films in the vicinity of the (103) substrate and LSCO film reflections. The contour plot is on a logarithmic scale and shows the scattered intensity as a function of the scattering vector q, expressed in noninteger Miller indices h and l of the substrate reflection. Peak positions for a fully relaxed LSCO layer are indicated by a cross. (b) ε_{xx} (open symbols) and ε_{zz} (filled symbols) versus a_s at room temperature. The bulk lattice parameter $a_0$of LSCO is indicated by the arrow. (c) ε_{zz} versus ε_{xx}. The solid line is a linear fit to the data. (d) Magnetic moment m versus T for $\mu_0 H = 20$ mT and (e) m versus $\mu_0 H$ with magnetic field applied parallel to the film surface.

In Fig. 2, the O K absorption and XMCD spectra of strained LSCO films are displayed for normal and grazing incidence. In the energy range shown in Figs. 2(b) and 2(d), the spectra reflect the unoccupied O $2p$ density of states hybridized with Co $3d$ eg and t_{2g} orbitals. A strong peak centered around 528 eV is found in the absorption data. This feature corresponds predominantly to unoccupied states in the t_{2g} spectral range. The large spectral weight (SW) at 528 eV indicates a large number of unoccupied t_{2g}-derived states—typical for a dominant HS configuration and well in consistence with the results obtained from multiplet calculations and the Co $L_{2,3}$ absorption edge spectra [24].

The O K XMCD spectra displayed in the lower part of Fig. 2 show a strong negative peak only in the t_{2g} spectral range. Due to the absence of spin-orbit splitting for an $1s$ core level, the O K edge XMCD spectra display merely the orbital moment but are insensitive to the spin moment [25]. Accordingly, for LSCO, the t_{2g} feature in XMCD reflects the transfer of a t_{2g} electron's orbital moment from the Co to the O site, enabling double exchange between Co^{3+} HS and Co^{4+} HS [12].

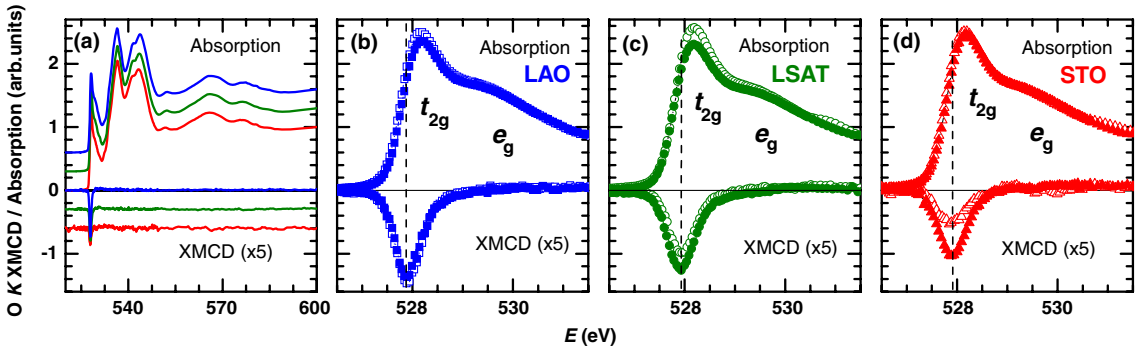

FIG. 2 (color online). O K absorption and XMCD of LSCO films on LAO, LSAT, and STO, taken at 20 K from top to bottom (a) and left to right (b)–(d), respectively. (a) Survey of the spectra recorded at normal incidence from 520–600 eV. The spectra are shifted for clarity. (b)–(d) Spectra recorded at normal incidence (open symbols) and at grazing incidence (filled symbols). An XMCD effect, indicated by the dashed line, is found only in the energy range where the unoccupied O $2p$ density of states is predominantly hybridized with Co $3d$ t_{2g} orbitals.

In accordance with the magnetization measurements, a profound strain dependence of the magnetic anisotropy is found. For tensile-strained LSCO on LSAT and STO, the XMCD signal is larger for grazing than for normal incidence, indicating orbital moments essentially oriented within the film plane. For compressive-strained films on LAO, the situation is reverse. The anisotropy increases with increasing ε_{xx} and indicates that the states contributing most strongly to the in-plane and out-of-plane orbital moment, i.e., t_{2g}-derived d_{xy}, d_{xz}, and d_{yz} states, are not equally occupied. Usually tensile strain leads to a lowering of the energy of d_{xy}-derived states. Since the electronic t_{2g} configurations of Co^{3+} LS ($6t_{2g}$ $0e_g$) and Co^{4+} HS ($3t_{2g}$ $2e_g$) are not Jahn-Teller (JT) active, the magnetic anisotropy is restricted to Co^{3+} HS ($4t_{2g}$ $2e_g$) only, which further indicates the Co^{3+}HS/Co^{4+} HS t_{2g} double exchange in LSCO.

Although the energetic splitting of the t_{2g}-derived states is too small to be resolved in the absorption spectra, the different orbital occupation clearly indicates the JT distortion imposed by epitaxial strain in contrast to bulk LSCO which does not display a measurable JT splitting [26].

In the following, we relate the magnetic and electronic properties of LSCO directly to the strain. The standard model to describe magnetism in perovskite related TM oxides is the DE mechanism described by Zener and de Gennes [10,11]. In the strong-coupling limit ($J_{ex} \gg W$), the model predicts the magnitude of the DE to be proportional to the electron transfer integral t, i.e., the bandwidth W [27], resulting in $T_C \propto W$. Epitaxial strain affects the TM-O bond length d or the TM-O-TM bonding angle β and hence, W and T_C. Millis *et al.* [28,29] have shown that polaronic effects due to strong electron-phonon coupling arising from JT splitting of the Mn^{3+} ions have to be considered as well to explain the physical properties of manganites. Hence, pressure and epitaxial strain leading to octahedral distortion or deformation may influence T_C significantly. We, therefore, follow the approach of Millis *et al.* [30]. For weak strain in a cubic system, T_C can be expanded in powers of strain as

$$T_C(\varepsilon_B, \varepsilon_{JT}) = T_{C0}(1 + \alpha\varepsilon_B - D\varepsilon_{JT}^2/2), \quad (1)$$

with the coefficients $\alpha = (1/T_C)dT_C/d\varepsilon_B$ and $D = (1/T_C)d^2T_C/d\varepsilon_{JT}^2$, the bulk compression $\varepsilon_B = -(\varepsilon_{xx} + \varepsilon_{yy} + \varepsilon_{zz})/3$, the isotropic biaxial Jahn-Teller distortion $\varepsilon_{JT} = (\varepsilon_{zz} - \varepsilon_{xx})/2$, and the Curie temperature T_{C0} for unstrained conditions. For $\varepsilon_{zz} = c^* - \varepsilon_{xx}$ and $\varepsilon_{yy} = \varepsilon_{xx}$, this leads to

$$T_C = A + B\varepsilon_{xx} + C\varepsilon_{xx}^2, \quad (2)$$

with $A = T_{C0}(1 - \alpha c^*/3 - Dc^{*2}/8)$, $B = T_{C0}(Dc^*/2 - \alpha/3)$, and $C = -T_{C0}(D/2)$. Figure 3(a) displays T_C as a function of ε_{xx}. A polynomial fit to the data corresponding to Eq. (2) is shown by the solid line. The fit clearly demonstrates that besides the linear term coming from the bulk compression, a quadratic term due to the JT distortion is present as well. From the fit, we obtain $T_{C0} \approx 221$ K, $D \approx 700$, and $\alpha \approx 11.8$. The data point for unstrained polycrystalline LSCO is displayed as well. Note that because of the residual strain c* along the c axis, $T_C(\varepsilon_{xx} = 0)$ is reduced with respect to T_{C0}. T_{C0} agrees very well with T_C of polycrystalline LSCO. For compressively strained films on LAO ($\varepsilon_B > 0$), the increase of T_C due to the bulk compression is overcompensated by ε_{JT} yielding a T_C lower than the vertex of $T_C(\varepsilon_{xx})$. The JT distortion is visualized likewise in Fig. 3(b), where the difference between integrated normal and grazing incidence O K XMCD, i.e., Δ(O K XMCD) = O K XMCD$^{\perp}$ − O K XMCD$^{\parallel}$, is shown versus ε_{xx}. With increasing tensile strain, O K XMCD$^{\parallel}$ increases and O K XMCD$^{\perp}$ decreases, leading to isotropic behavior for $\varepsilon_{xx} = 0$.

Figure 3(a) displays, in addition to $T_C(\varepsilon_{xx})$, the integrated XMCD signal averaged over the out-of-plane and in-plane directions, i.e., $\langle$O K XMCD$\rangle$ = (O K XMCD$^{\perp}$ + O K XMCD$^{\parallel}$)/2 versus ε_{xx}. $\langle$O K XMCD$\rangle$ is indicative of

the transfer of a t_{2g} electron's orbital moment from the Co to the O site and thus, provides a reasonable measure for the magnetic exchange. Obviously, $\langle$O K XMCD$\rangle$ shows nearly the same dependence on ε_{xx} as T_C, demonstrating a nearly linear correlation between T_C and $\langle$O K XMCD$\rangle$ in agreement with what is expected for double exchange in the strong-coupling limit.

Figures 3(a) and 3(b) clearly show that T_C is obviously affected by the presence of $\varepsilon_{\mathrm{JT}}$ and provide evidence for the relevance of JT electron-phonon coupling in doped cobaltates. The coefficient D expressing the sensitivity of T_C to $\varepsilon_{\mathrm{JT}}$ is by a factor 2–3 smaller than that observed for $La_{0.7}Sr_{0.3}MnO_3$ (LSMO) films [31,32]. This can be understood qualitatively if the JT activity of the involved TMs is compared. In LSMO, the energy gain by the JT splitting of e_g-derived Mn^{3+} states amounts to about 0.75 eV [33]. For the cobaltates, only Co^{3+} HS ($4t_{2g}$ $2e_g$) ions—restricted to t_{2g}-derived states—are JT active. For LSCO, the XMCD signals, shown in Fig. 2, for normal and grazing incidence do not indicate an energy splitting of d_{xz}-, d_{yz}-, and d_{xy}-derived states. A possible change in JT splitting would manifest itself in a small O K XMCD peak shift of the order of Δ_{JT}. Even in the presence of larger intrinsic broadening effects, absolute peak shifts can be determined here to 0.15 eV or better, giving an estimated upper limit for Δ_{JT} which is a factor of 5 smaller compared to manganites.

On the other hand, the effect of bulk compression on T_C is about twice as large for cobaltates. For strained LSMO films, $\alpha \approx 6$ has been reported [32,34]. The bulk coefficient α can be likewise derived from the pressure dependence of T_C and the volume compressibility, i.e., $\alpha = (-3/T_C) \times (dT_C/dp)Vdp/dV$ [30]. For comparison, Fig. 3(c) shows $(1/T_C)dT_C/dp$ for $La_{1-x}Sr_xCoO_3$ and $La_{1-x}Sr_xMnO_3$ as a function of x. The data were taken from Refs. [35,36]. The bulk moduli of the materials are comparable and amount to about 150 GPa [37,38]. Cobaltates and manganites obviously display a completely reverse behavior. For manganites, $(1/T_C)dT_C/dp$ is always positive—typical for double exchange—however, clearly decreasing with increasing hole doping which drives the system to the weak-coupling region with lower sensitivity to pressure or W [36]. For cobaltates, $(1/T_C)dT_C/dp$ increases with increasing x and becomes larger compared to the manganites for $x \geq 0.3$ [39]. Negative values of $(1/T_C)dT_C/dp$ are caused by the spin- or cluster-glass phase. The enhanced strong-coupling behavior of cobaltates can be explained by the smaller quasiparticle bandwidth of the t_{2g}-derived states [40]—responsible for the magnetic exchange in cobaltates—compared to the larger W of e_g-derived states in the case of manganites.

The values for α and D obtained from the fit in Fig. 3(a) are, therefore, quite conclusive even though the number of strain systems might seem small.

In summary, we have investigated the magnetic exchange in hole-doped LSCO films by studying the magnetic and electronic properties as a function of epitaxial strain. The O K XMCD signal reflects the transfer of a t_{2g} electron's orbital moment from the Co to the O site concomitant with the DE between Co^{3+} HS and Co^{4+} HS states. The strain-induced shift of T_C as well as the difference between normal and grazing incidence O K XMCD convincingly show that besides the bulk compression ε_{B} the strain-induced biaxial lattice distortion, $\varepsilon_{\mathrm{JT}}$, plays a prominent role. The large sensitivity of T_C to ε_{B} indicates that double exchange approaches the limit of strong coupling. The latter is substantiated by the linear correlation between T_C and the strength of the O2p-Co3d hybridization. The strong-coupling behavior can be explained by the small bandwidth of the t_{2g}-derived states. The drastically different dependence of T_C on the bulk compression of cobaltates and manganites unveiled in the present Letter requires further theoretical and experimental scrutiny.

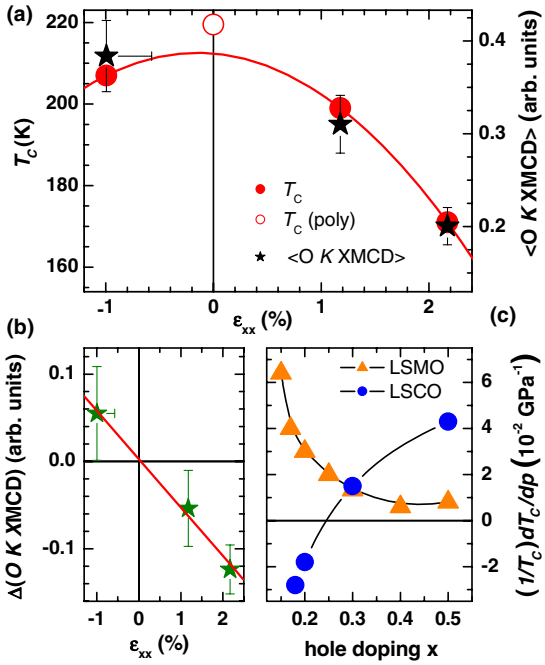

FIG. 3 (color online). (a) T_C (circles) and averaged O K XMCD (stars) of LSCO films versus ε_{xx}. The line is a fit of Eq. (2) to the T_C data of the strained films. The T_C of polycrystalline unstrained LSCO is displayed by the open circle. (b) The difference between normal and grazing incidence O K XMCD, $\Delta(\mathrm{O}\,K\,\mathrm{XMCD}) = \mathrm{O}\,K\,\mathrm{XMCD}^{\perp} - \mathrm{O}\,K\,\mathrm{XMCD}^{\parallel}$, versus ε_{xx}. The line is a linear fit to the data. (c) $(1/T_C)dT_C/dp$ for $La_{1-x}Sr_xCoO_3$ (circles) and $La_{1-x}Sr_xMnO_3$ (triangles) as a function of x. The data were taken from Refs. [35,36]. Lines are guide to the eye.

[1] M. Itoh, I. Natori, S. Kubota, and K. Motoya, J. Phys. Soc. Jpn. **63**, 1486 (1994).
[2] J. Wu and C. Leighton, Phys. Rev. B **67**, 174408 (2003).
[3] C. He, M. A. Torija, J. Wu, J. W. Lynn, H. Zheng, J. F. Mitchell, and C. Leighton, Phys. Rev. B **76**, 014401 (2007).

[4] M. A. Senaris-Rodriguez and J. B. Goodenough, J. Solid State Chem. **116**, 224 (1995).

[5] D. Fuchs, C. Pinta, T. Schwarz, P. Schweiss, P. Nagel, S. Schuppler, R. Schneider, M. Merz, G. Roth, and H. v. Löhneysen, Phys. Rev. B **75**, 144402 (2007).

[6] D. Fuchs, E. Arac, C. Pinta, S. Schuppler, R. Schneider, and H. v. Löhneysen, Phys. Rev. B **77**, 014434 (2008).

[7] C. Pinta, D. Fuchs, M. Merz, M. Wissinger, E. Arac, H. v. Löhneysen, A. Samartsev, P. Nagel, and S. Schuppler, Phys. Rev. B **78**, 174402 (2008).

[8] D. Fuchs, L. Dieterle, E. Arac, R. Eder, P. Adelmann, V. Eyert, T. Kopp, R. Schneider, D. Gerthsen, and H. v. Löhneysen, Phys. Rev. B **79**, 024424 (2009).

[9] J. B. Goodenough, J. Phys. Chem. Solids **6**, 287 (1958).

[10] C. Zener, Phys. Rev. **82**, 403 (1951).

[11] P. G. de Gennes, Phys. Rev. **118**, 141 (1960).

[12] M. Merz, P. Nagel, C. Pinta, A. Samartsev, H. v. Löhneysen, M. Wissinger, S. Uebe, A. Assmann, D. Fuchs, and S. Schuppler, Phys. Rev. B **82**, 174416 (2010).

[13] S. Medling, Y. Lee, H. Zheng, J. F. Mitchell, J. W. Freeland, B. N. Harmon, and F. Bridges, Phys. Rev. Lett. **109**, 157204 (2012).

[14] M. A. Señaríz-Rodríguez and J. B. Goodenough, J. Solid State Chem. **118**, 323 (1995).

[15] D. Fuchs, T. Schwarz, O. Morán, P. Schweiss, and R. Schneider, Phys. Rev. B **71**, 092406 (2005).

[16] D. Fuchs, P. Schweiss, P. Adelmann, T. Schwarz, and R. Schneider, Phys. Rev. B **72**, 014466 (2005).

[17] R. Caciuffo, D. Rinaldi, G. Barucca, J. Mira, J. Rivas, M. A. Senaris-Rodriguez, P. G. Radaelli, D. Fiorani, and J. B. Goodenough, Phys. Rev. B **59**, 1068 (1999).

[18] M. Kriener, C. Zobel, A. Reichl, J. Baier, M. Cwik, K. Berggold, H. Kierspel, O. Zabara, A. Freimuth, and T. Lorenz, Phys. Rev. B **69**, 094417 (2004).

[19] H. M. Aarbogh, J. Wu, L. Wang, H. Zheng, J. F. Mitchell, and C. Leighton, Phys. Rev. B **74**, 134408 (2006).

[20] From the intensity distribution, it can be estimated in a worst case scenario that 79% of the film volume are fully strained and 21% are relaxed to $\varepsilon_{xx} = -0.57\%$ and $\varepsilon_{zz} = 0.68\%$. Error bars were set with respect to these values.

[21] J. O'Donnell, M. S. Rzchowski, J. N. Eckstein, and I. Bozovic, Appl. Phys. Lett. **72**, 1775 (1998).

[22] T. K. Nath, R. A. Rao, D. Lavric, C. B. Eom, L. Wu, and F. Tsui, Appl. Phys. Lett. **74**, 1615 (1999).

[23] L. M. Berndt, V. Balbarin, and Y. Suzuki, Appl. Phys. Lett. **77**, 2903 (2000).

[24] M. Merz, D. Fuchs, A. Assmann, S. Uebe, H. v. Löhneysen, P. Nagel, and S. Schuppler, Phys. Rev. B **84**, 014436 (2011).

[25] The strain-dependent behavior of the in- and out-of-plane orbital moments deduced from the O K edge spectra compare well with those extracted from the Co $L_{2,3}$ edge spectra, i.e., $m_{\mathrm{orb}}^{\perp} = 0.357$, 0.273, and 0.198 μ_B/Co and $m_{\mathrm{orb}}^{||} = 0.319$, 0.338, and 0.3 μ_B/Co for LSCO films on LAO, LSAT, and STO, respectively.

[26] Y. Jiang, F. Bridges, N. Sundaram, D. P. Belanger, I. E. Anderson, J. F. Mitchell, and H. Zheng, Phys. Rev. B **80**, 144423 (2009).

[27] P. W. Anderson and H. Hasegawa, Phys. Rev. **100**, 675 (1955).

[28] A. J. Millis, P. B. Littlewood, and B. I. Shraiman, Phys. Rev. Lett. **74**, 5144 (1995).

[29] A. J. Millis, R. Mueller, and B. I. Shraiman, Phys. Rev. B **54**, 5405 (1996).

[30] A. J. Millis, T. Darling, and A. Migliori, J. Appl. Phys. **83**, 1588 (1998).

[31] Y. Lu, J. Klein, C. Hofener, B. Wiedenhorst, J. B. Philipp, F. Herbstritt, A. Marx, L. Alff, and R. Gross, Phys. Rev. B **62**, 15806 (2000).

[32] C. Thiele, K. Dörr, O. Bilani, J. Rödel, and L. Schultz, Phys. Rev. B **75**, 054408 (2007).

[33] S. Satpathy, Z. S. Popovic, and F. R. Vukajlovic, J. Appl. Phys. **79**, 4555 (1996).

[34] F. Tsui, M. C. Smoak, T. K. Nath, and C. B. Eom, Appl. Phys. Lett. **76**, 2421 (2000).

[35] I. Fita, R. Szymczak, R. Puzniak, I. O. Troyanchuk, J. Fink-Finowicki, Ya. M. Mukovskii, V. N. Varyukhin, and H. Szymczak, Phys. Rev. B **71**, 214404 (2005).

[36] Y. Moritomo, A. Asamitsu, and Y. Tokura, Phys. Rev. B **51**, 16491 (1995).

[37] T. Vogt, J. A. Hriljac, N. C. Hyatt, and P. Woodward, Phys. Rev. B **67**, 140401 (2003).

[38] T. W. Darling, A. Migliori, E. G. Moshopoulou, S. A. Trugman, J. J. Neumeier, J. L. Sarrao, A. R. Bishop, and J. D. Thompson, Phys. Rev. B **57**, 5093 (1998).

[39] The $La_{0.7}Sr_{0.3}Co_3$ sample of Fita *et al.* showed a T_C of 212 K, smaller compared to T_C of our sample. Thus, the hole doping is assumed to be smaller shifting the $(1/T_C)dT_C/dp$ for $x = 0.3$ to higher values.

[40] P. Augustinský, V. Křápek, and J. Kuneš, Phys. Rev. Lett. **110**, 267204 (2013).